# Omnidirectional Measurements of Angle-Resolved Heat Capacity for Complete Detection of Superconducting Gap Structure in the Heavy-Fermion Antiferromagnet $UPd_2Al_3$

Yusei Shimizu,[1,*] Shunichiro Kittaka,[1] Toshiro Sakakibara,[1] Yasumasa Tsutsumi,[2] Takuya Nomoto,[3] Hiroaki Ikeda,[4] Kazushige Machida,[4] Yoshiya Homma,[5] and Dai Aoki[5]
[1]*Institute for Solid State Physics (ISSP), The University of Tokyo, Kashiwa, Chiba 277-8581, Japan*
[2]*Department of Basic Science, The University of Tokyo, Meguro, Tokyo 153-8902, Japan*
[3]*Departement of Physics, Kyoto University, Kyoto 606-8502, Japan*
[4]*Department of Physics, Ritsumeikan University, Kusatsu, Shiga 525-8577, Japan*
[5]*Institute for Materials Research, Tohoku University, Oarai, Ibaraki 311-1313, Japan*
(Received 13 March 2016; published 12 July 2016)

Quasiparticle excitations in $UPd_2Al_3$ were studied by means of heat-capacity ($C$) measurements under rotating magnetic fields using a high-quality single crystal. The field dependence shows $C(H) \propto H^{1/2}$-like behavior at low temperatures for both two hexagonal crystal axes, i.e., $H\|[0001]$ ($c$ axis) and $H\|[11\bar{2}0]$ ($a$ axis), suggesting the presence of nodal quasiparticle excitations from heavy bands. At low temperatures, the polar-angle ($\theta$) dependence of $C$ exhibits a maximum along $H\|[0001]$ with a twofold symmetric oscillation below 0.5 T, and an unusual shoulder or hump anomaly has been found around 30°–60° from the $c$ axis in $C(\theta)$ at intermediate fields ($1 \lesssim \mu_0 H \lesssim 2$ T). These behaviors in $UPd_2Al_3$ purely come from the superconducting nodal quasiparticle excitations, and can be successfully reproduced by theoretical calculations assuming the gap symmetry with a horizontal linear line node. We demonstrate the whole angle-resolved heat-capacity measurements done here as a novel spectroscopic method for nodal gap determination, which can be applied to other exotic superconductors.

DOI: 10.1103/PhysRevLett.117.037001

The successive discoveries of heavy-fermion superconductivity in $CeCu_2Si_2$, $UBe_{13}$, $UPt_3$, and $URu_2Si_2$ [1–4], opened up a frontier for exploring an unconventional pairing mechanism. Afterward, it was found that isostructural compounds $UPd_2Al_3$ and $UNi_2Al_3$ show the coexistence of unconventional superconductivity and a long-range antiferromagnetic (AF) order [5,6]. $5f$-electron superconductivity has been frequently observed in the vicinity of or coexistent with an inherent long-range order [1–4], as is the case of the above two AF superconductors [5,6]. Moreover, unconventional superconductivity coexists with the hidden-ordered state in $URu_2Si_2$ [4], and ferromagnetic order in $UGe_2$, URhGe, and UCoGe [7–9]. These facts imply that nonphononic interactions associated with these ordered phases play dominant roles in forming Cooper pairs.

In this Letter, we focus on the superconducting (SC) gap symmetry of $UPd_2Al_3$, which crystallizes in the hexagonal structure with the space group $P6/mmm$. Below $T_N \sim 14.5$ K, the ordered moment $\sim 0.85\mu_B/\mathrm{U}$ with the wave vector $\boldsymbol{Q}_0 = (0, 0, 1/2)$ aligns antiferromagnetically along [0001] and ferromagnetically in the hexagonal basal plane [10]. The SC transition occurs at $T_c \sim 2.0$ K with a large specific-heat jump [5,11], indicating an intrinsic participation of $5f$ heavy electrons. The interplay between the AF and SC states has been suggested from tunnel-junction [12] and inelastic neutron-scattering studies [13–16].

$UPd_2Al_3$ is a typical $5f$ system in which the $5f$ electron exhibits duality, the localized and itinerant natures. On the one hand, the anisotropic magnetic susceptibility $\chi(T)$ as well as the heat capacity are well explained by the crystalline-electric-field level scheme for localized $5f^2$ electrons ($U^{4+}$, $J = 4$) [17]. Furthermore, at the AF transition, the $5f$ electron releases a large entropy ($\sim 0.7R \ln 2$), indicating that the $5f$ electrons have a well-localized character [17]. On the other hand, the heavy cyclotron effective masses of 5–65$m_0$ ($m_0$: the free-electron mass) are observed from de Haas–van Alphen (dHvA) measurements [18,19]. The observed heavy bands are well explained by band calculations based on the $5f$ itinerant model [19–22]. Given the fact that there are only a few $5f$ heavy-electron superconductors whose Fermi surfaces have been well established, $UPd_2Al_3$ is an ideal system for understanding how the originally localized $5f$ electrons acquire the itineracy with a huge effective mass and form Cooper pairs overcoming the strong repulsions.

To understand the pairing mechanism, it is important to clarify the SC gap symmetry, since it reflects the momentum dependence of the pairing interaction. The NMR Knight shift and the NMR/ nuclear-quadrupole-resonance (NQR) spin-relaxation rate ($1/T_1 \propto T^3$) have clearly shown the even-parity SC state with line node(s) [23,24]. The inelastic neutron-scattering studies have proposed the possibility of the gap function with nodal $A_{1g}$ symmetry, $\Delta(\boldsymbol{k}) = \Delta_0 \cos(k_z c)$, which satisfies $\Delta(\boldsymbol{k}) = -\Delta(\boldsymbol{k} + \boldsymbol{Q}_0)$ [25] and exhibits sign changes of the gap function (line nodes) at the AF Brillouin zone boundary

 

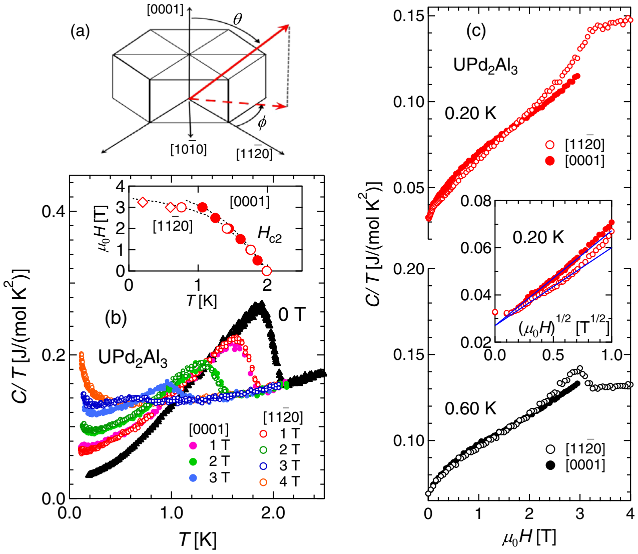


FIG. 1. (a) The definition of azimuthal ($\phi$) and polar ($\theta$) angles for the hexagonal structure, where the $\phi$ and $\theta$ are measured from [11$\bar{2}$0] and [0001] axes, respectively. (b) Temperature dependence of $C/T$ in $UPd_2Al_3$, measured at 0, 1, 2, and 3 T for $H\|[0001]$ and $H\|[11\bar{2}0]$. For $H\|[11\bar{2}0]$, we also plot the data at 4 T with no SC transition. The inset shows $H_{c2}$, obtained from temperature scans $C(T)$ for $H\|[0001]$ (closed circle) and $H\|[11\bar{2}0]$ (open circle). The diamond marker indicates $H_{c2}$, obtained from field scans $C(H)$ for $H\|[11\bar{2}0]$. (c) Magnetic-field dependence of $C/T$ for $H\|[0001]$ and $H\|[11\bar{2}0]$, measured at 0.20 and 0.60 K. The inset shows $C(H)/T$ measured at 0.20 K as a function of $H^{1/2}$ for $H\|[0001]$ and $H\|[11\bar{2}0]$, where solid lines are the results of linear fitting at low-field region.

$k_z = \pm(\pi/2c)$, where $\Delta_0$ and $c$ are the gap amplitude and the $c$-axis lattice constant [14,15]. Furthermore, the precise thermal-conductivity measurements have also supported the presence of horizontal line nodes [26]. However, a thermodynamic evidence for the horizontal line node in heavy bands has not yet been established.

In order to examine the pairing symmetry of $UPd_2Al_3$ from the point of view of the heavy-electron density of states, we studied the low-energy quasiparticle excitations by means of heat-capacity measurements down to ∼0.1 K in magnetic fields up to 4 T. The heat capacity was measured by the thermal-relaxation methods in a dilution refrigerator, and its field-orientation dependence $C(H,\phi,\theta)$ was measured with rotating magnetic fields using a 5 T × 3 T vector magnet as shown in Fig. 1(a), where the azimuthal and polar angles $\phi$ and $\theta$ are measured from the [11$\bar{2}$0] and [0001], respectively. A single crystalline $UPd_2Al_3$ (4.13 mg) with the residual-resistivity ratio of 99 was prepared by the Czochralski pulling method in a tetra-arc furnace. The high quality was ensured by the dHvA oscillations in the dc magnetization measurements for the present sample.

Figure 1(b) shows temperature dependencies of $C/T$, measured at 0, 1, 2, and 3 T for $H\|[0001]$ and $H\|[11\bar{2}0]$. The SC transition temperature is $T_c \sim 2.0$ K at zero field. For $H\|[11\bar{2}0]$, we also plot the data measured at 4 T, which is larger than the upper critical field. The upturn of $C/T$ at low temperatures in magnetic fields comes from the nuclear contribution.

Magnetic-field dependence of the heat capacity and its anisotropy in low fields are useful to probe quasiparticle excitations around nodes. In the case of a line node, for instance, $C(H)$ exhibits $H^{1/2}$-like (concave upward) behavior at low $T$ [27,28]. Moreover, this $H^{1/2}$ dependence is predicted to be slightly anisotropic depending on the angle between $H$ and the nodal direction [28–30]. The field-angular variation of $C(H)$ has indeed been observed in nodal superconductors [31,32]. As can be seen in Fig. 1(c), the field variation of the heat capacity [$C(H)$] in the SC state well below $T_c$ shows $H^{1/2}$-like curvature. Importantly, this $H^{1/2}$-like behavior is anisotropic between [0001] and [11$\bar{2}$0] directions; $C_{[0001]}(H)$ for $H\|[0001]$ is larger than $C_{[11\bar{2}0]}(H)$ for $H\|[11\bar{2}0]$ below ∼1.5 T, as will be shown more clearly in Figs. 3(a) and 3(b). Both the amplitude of the $H^{1/2}$-like behavior and its anisotropy become more pronounced at 0.20 K ($= 0.1T_c$) than at 0.60 K ($= 0.3T_c$).

In a high-field region above ∼2 T [Fig. 1(c)], the anisotropy of $C(H)$ is reversed: $C_{[0001]}(H) < C_{[11\bar{2}0]}(H)$. This anisotropy reversal reflects the anisotropy of the upper critical field $H_{c2}$. Because of the present experimental limitation, the maximum field for $H\|[0001]$ was 3 T, slightly lower than $H_{c2}$ in this direction. For $H\|[11\bar{2}0]$, $C(H)/T$ at 0.20 K shows a kink at $H_{c2} \sim 3.3$ T. Note that $C_{[11\bar{2}0]}(H)/T$ in the SC state at $T = 0.20$ K exhibits an upturn in the high-$H$ region, reminiscent of a strong Pauli paramagnetic effect as observed in $CeCoIn_5$ [33]. The presence of the paramagnetic effect for $UPd_2Al_3$ is consistent with the results of NMR Knight-shift measurements, which points to an even-parity pairing [24].

The inset of Fig. 1(b) shows $H_{c2}(T)$ obtained from the $C(T)$ and $C(H)$ data. The initial slope of $H_{c2}(T)$ is almost the same between [0001] and [11$\bar{2}$0], indicating the averaged Fermi velocity $\boldsymbol{v}_F$ is not so different for both directions, although the Fermi surface is rather complicated [19–22]. Nevertheless, $H_{c2}(T)$ is evidently anisotropic at low $T$. This fact suggests that the paramagnetic limitation is anisotropic, reflecting the normal-state magnetic anisotropy between [0001] and [11$\bar{2}$0] directions [17].

To search for vertical line nodes, we measured the heat capacity by rotating fields in the hexagonal basal plane. Figures 2(a) and 2(b) show $C(\phi)/T$ in various magnetic fields measured at 0.20 and 0.60 K, respectively. As can be seen in Fig. 2, in a field of 2 T, we observe a sixfold oscillation with a maximum at $\phi = 30°$ ($H\|[10\bar{1}0]$) and a minimum at $\phi = 0°$ ($H\|[11\bar{2}0]$). This sixfold oscillation is most pronounced at 3 T and 0.20 K, and can be attributed to the in-plane anisotropy of the Fermi velocity and $H_{c2}$, as observed in thermal conductivity [26,34]. In a normal state at 4 T and 0.20 K, another small sixfold oscillation with a

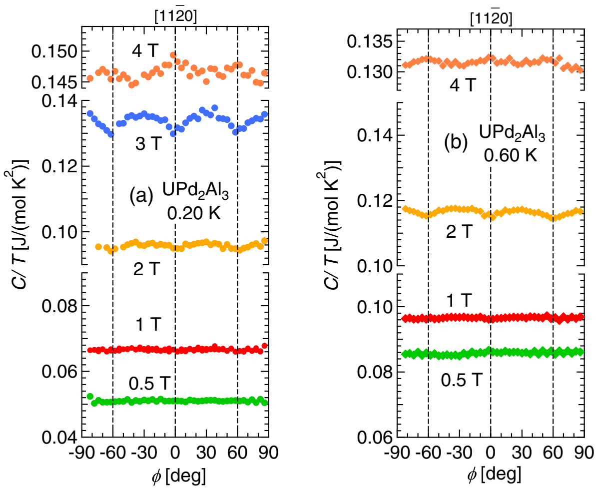


FIG. 2. Azimuthal angle dependence of the heat capacity $C(\phi)/T$ in $UPd_2Al_3$ in the hexagonal basal plane, measured in various fields at (a) 0.20 K and (b) 0.60 K. The scale of the vertical axes are enlarged for 4 T.

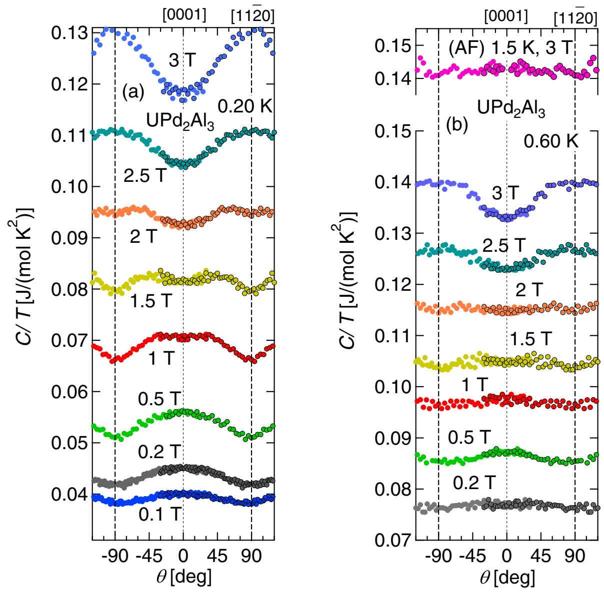


FIG. 3. The field-angle dependence $C(\theta)/T$ of $UPd_2Al_3$ within the $ac$ plane in various fields, measured at (a) 0.20 and (b) 0.60 K. In these plots, the measurements of $C(\theta)$ were done in the range from $\theta = -30°$ to $\theta = 120°$ (symbols with black border), and the mirrored copy with respect to $\theta = 0°$ is overlaid (symbols without black border) to show the twofold symmetry more clearly. We plot in (b) the data measured in the (AF ordered) normal state at 1.5 K and 3 T.

maximum (minimum) at 0° (30°) is seen, becoming weaker at 0.60 K. This oscillation is attributed to the AF domain structure [26,34]. At a low temperature (0.20 K) and low field (0.5 T) region, no significant oscillation is observed, being consistent with the absence of vertical line nodes as reported from the angle-resolved thermal-conductivity measurements [26].

To probe the horizontal line node, we further examined the polar-angle ($\theta$) dependence of the heat capacity $C(\theta)$. Thanks to the weak anisotropy of the Fermi velocity, there is a good chance to detect the quasiparticle excitations around the horizontal line node by $C(\theta)$ measurements, in spite of the hexagonal structure. In Figs. 3(a) and 3(b), we show $C(\theta)/T$ measured in various fields at 0.20 and 0.60 K ($\phi = 0°$). Below 0.5 T, a twofold oscillation is clearly observed with a maximum at $\theta = 0°$ ($H \| [0001]$) and a minimum at $\theta = 90°$ ($H \| [11\bar{2}0]$). The magnitude of the observed anisotropy at 0.5 T is $\Delta C/C_{\mathrm{mid}} \sim 6.8\%$ and 2.0% at 0.20 K and 0.60 K, respectively, where $\Delta C \equiv C(\theta = 0°) - C(\theta = 90°)$ and $C_{\mathrm{mid}} \equiv [C(\theta = 0°) + C(\theta = 90°)]/2$. Above 2.5 T, the twofold angular oscillation is reversed and the maximum appears along $[11\bar{2}0]$, reflecting the underlying nodal structure as well as the anisotropy of $H_{c2}$.

Very interestingly, in the field range from 1 to 2 T, a new feature appears in $C(\theta)$ in an intermediate angle region, becoming more distinct with decreasing $T$ [Figs. 3(a) and 3(b)]. For 0.20 K at 1 T, a shoulder or a hump appears at $\theta \sim 30°$, and moves to the higher angle side $\theta \sim 45°$–$60°$ with increasing $H$ from 1.5 and 2 T. This feature can still be seen at 0.60 K in the field range 1.5–2 T. Above 2.5 T, it finally merges into the maximum at $\theta = 90°$ arising from the $H_{c2}$ anisotropy. Remarkably, the maximum of $C(\theta)/T$ at 1.5 T occurs near 45°; $C(\theta = 45°)$ is larger than $C(\theta = 90°)$ and $C(\theta = 0)$. Such a shoulder or hump feature hardly arises from the anisotropy of Fermi velocity [36]. It should also be noticed that there is no significant angular dependence of $C(\theta)$ in the normal (AF) state above $H_{c2}$ [Fig. 3(b)]. We thus conclude that the shoulder or hump anomaly purely comes from the quasiparticle excitations reflecting the nodal SC gap.

We argue that the observed field evolution of $C(\theta)$, i.e., the sign reversal of the twofold oscillation as well as the shoulder or hump structure in the intermediate angular region, provides strong evidence that a horizontal line node exists on the Fermi surface at which $\boldsymbol{v}_F$ is perpendicular to $z$. Let us consider the zero-energy density of states (ZEDOS) arising from the Doppler shift $\delta E \propto \boldsymbol{v}_s \cdot \boldsymbol{v}_F$ of nodal quasiparticle excitations due to the supercurrent circulating around the vortices [27], where $\boldsymbol{v}_s$ denotes the superfluid velocity ($\boldsymbol{v}_s \perp H$). At low fields, $\delta E$ is clearly the largest for $\theta = 0$ because all the nodal quasiparticles can contribute. For $\theta = 90°$, by contrast, those nodal quasiparticles whose $\boldsymbol{v}_F$ is perpendicular to $\boldsymbol{v}_s$ are not Doppler shifted and cannot contribute to the ZEDOS. As a result, the induced ZEDOS takes maximum (minimum) at $\theta = 0°$ ($\theta = 90°$). This twofold angular dependence of the ZEDOS explains the angular variation of $C(\theta)/T$ at low fields.

In a high-field region, the $H_{c2}$ anisotropy contributes more to the $C(\theta)/T$ because $C(\theta)/T \propto [H/H_{c2}(\theta)]^{\beta}$ [36]. Generally, $H_{c2}$ is the lowest for the nodal direction ($\theta = 90°$ in the present case). As a consequence, $C(\theta)/T$ is expected to take the maximum at $\theta = 90°$ in high fields, as observed in Fig. 3(a).

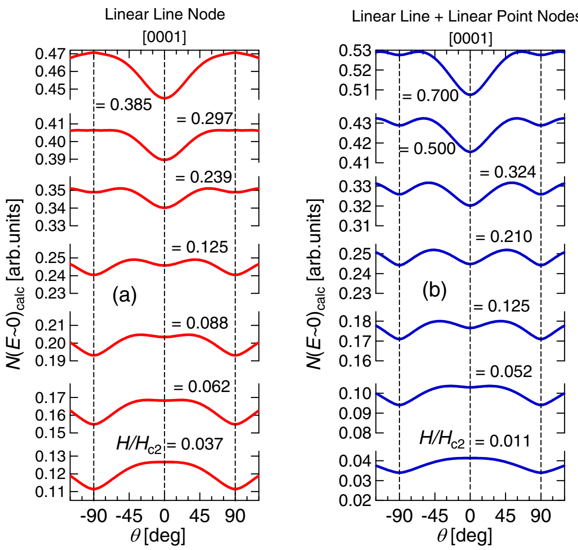


FIG. 4. Calculated results of the field-angle dependence of ZEDOS (arb. units) in magnetic fields normalized by $H_{c2}$ for (a) a linear horizontal line node and (b) a linear horizontal line and point nodes at the poles, respectively.

A crucial question is whether the horizontal line node can also explain the shoulder or hump anomaly in $C(\theta)$ at $\theta = 30°$–$45°$ observed in the intermediate range from 1 to 2 T [Fig. 3(a)]. To address this question, we performed microscopic calculations of the ZEDOS by means of the quasiclassical Eilenberger theory within the Kramer-Pesch approximation [37] whose qualitative validity was checked by Tsutsumi *et al.* [38]. Figure 4(a) shows the calculated angular dependence of ZEDOS, assuming a spherical Fermi surface and a model gap function $\Delta(\boldsymbol{k}) = \Delta_0 k_z$ that has a horizontal line node at the equator. The results clearly demonstrate that the anisotropy inversion occurs in the ZEDOS as $H$ increases. What is more important is that the calculated results successfully reproduce the shoulder or hump anomaly around 30°–60° in $C(\theta)$ at the intermediate fields. We confirmed that these features in the field evolution of ZEDOS anisotropy can also be obtained for an ellipsoidal Fermi surface, ensuring their robustness against the shape of the Fermi surface.

We also performed the calculations with a model gap function $\Delta(\boldsymbol{k}) = \Delta_0 k_z(k_x + ik_y)$, which has point nodes along the poles in addition to a horizontal line node, and the results are given in Fig. 4(b). The overall features of the field evolution of the ZEDOS anisotropy are nearly the same as those for the case in which a horizontal line node alone is present. The only difference can be seen in high fields; a weak dip occurs at $\theta = 90°$. Within the present experimental resolution, however, we cannot discern whether this tiny dip at $\theta = 90°$ exists in our $C(\theta)/T$ data.

The present experimental results, along with the microscopic calculations, strongly indicate that a horizontal line node exists in $UPd_2Al_3$. This conclusion is fully compatible with the $A_{1g}$ gap function $\Delta(\boldsymbol{k}) = \Delta_0 \cos(k_z c)$ proposed by previous experiments. We note, however, that the present $C(\theta)/T$ data alone cannot exclude the $E_{1g}$ type gap function $\Delta(\boldsymbol{k}) = \Delta_0 k_z(k_x + ik_y)$, which is also possible in the hexagonal structure ($D_{6h}$) [39,40].

Finally, we discuss the relationship between the possible gap structures and the Fermi surface of $UPd_2Al_3$. The previous dHvA experiments and the band calculations [19,21] have revealed that the Fermi surface consists of four sheets. Among these, the hole sheet called “party hat” ($m^* \sim 65m_0$) and the electron sheet called “column” ($m^* \sim 33m_0$) are the heaviest. Both of the gap functions, $\Delta(\boldsymbol{k}) = \Delta_0 k_z$ and $\Delta(\boldsymbol{k}) = \Delta_0 k_z(k_x + ik_y)$, have a horizontal line node on these sheets. It is noteworthy that the Fermi surface is missing along the $z$ direction in these principal sheets. This implies that even if the gap function has polar point nodes, they are hardly detected by the heat-capacity measurements that mainly probe the heaviest bands.

In conclusion, we investigated the SC quasiparticle excitations of the AF heavy-fermion superconductor $UPd_2Al_3$ by means of heat-capacity measurements on a high-quality single crystal. The low-$T$ anisotropy in $C(H) \propto H^{1/2}$ behavior and its angular dependence in low fields strongly indicate the presence of a horizontal line node. The most striking observation in the present study is the field evolution of the anisotropy in the polar angle dependence of the heat capacity $C(\theta)$, in particular the shoulder or hump anomaly that emerges at intermediate magnetic fields ($1 \lesssim H \lesssim 2$ T) arising from low-energy nodal quasiparticle excitations. These experimental results of $C(H, \theta)$ can be successfully reproduced by theoretical calculations assuming a horizontal line node. As demonstrated in this Letter, the polar angle dependence of $C(\theta)$ possesses sufficiently high resolution to detect the presence of the horizontal line node. The omnidirectional measurements of angle-resolved $C(H, \phi, \theta)$ will be a useful tool to elucidate the gap symmetry in various exotic superconductors.

We thank Y. Yanase, Y. Onuki, and K. Ishida for valuable discussions and comments. The present work was supported in part by JSPS KAKENHI Grants No. 15H05883 (J-Physics), No. 25103726, No. 26400360, No. 15H05745, No. 15K17715, No. 15J05698, No. 15H05884 (J-Physics), No. 15H05882 (J-Physics), No. 16H04006, No. 15J01476, and No. 15K05158.

*yuseishimizu@issp.u-tokyo.ac.jp

[1] F. Steglich, J. Aarts, C. D. Bredl, W. Lieke, D. Meschede, W. Franz, and H. Schäfer, Phys. Rev. Lett. **43**, 1892 (1979).
[2] H. R. Ott, H. Rudigier, Z. Fisk, and J. L. Smith, Phys. Rev. Lett. **50**, 1595 (1983).
[3] G. R. Stewart, Z. Fisk, J. O. Willis, and J. L. Smith, Phys. Rev. Lett. **52**, 679 (1984).
[4] W. Schlabitz, J. Baumann, B. Pollit, U. Rauchschwalbe, H. M. Mayer, U. Ahlheim, and C. D. Bredl, Z. Phys. B **62**, 171 (1986); T. T. M. Palstra, A. A. Menovsky, J. van den Berg,

A. J. Dirkmaat, P. H. Kes, G. J. Nieuwenhuys, and J. A. Mydosh, Phys. Rev. Lett. **55**, 2727 (1985); M. B. Maple, J. W. Chen, Y. Dalichaouch, T. Kohara, C. Rossel, M. S. Torikachvili, M. W. McElfresh, and J. D. Thompson, Phys. Rev. Lett. **56**, 185 (1986).
[5] C. Geibel, C. Schank, S. Thies, H. Kitazawa, C. D. Bredl, A. Böhm, M. Rau, A. Grauel, R. Caspary, R. Helfrich, U. Ahlheim, G. Weber, and F. Steglich, Z Phys. B Condens. Matter **84**, 1 (1991).
[6] C. Geibel, S. Thies, D. Kaczorowski, A. Mehner, A. Grauel, B. Seidel, U. Ahlheim, R. Helfrich, K. Petersen, C. D. Bredl, and F. Steglich, Z Phys. B Condens. Matter **83**, 305 (1991).
[7] S. S. Saxena, P. Agarwal, K. Ahilan, F. M. Grosche, R. K. W. Haselwimmer, M. J. Steiner, E. Pugh, I. R. Walker, S. R. Julian, P. Monthoux, G. G. Lonzarich, A. Huxley, I. Sheikin, D. Braithwaite, and J. Flouquet, Nature (London) **406**, 587 (2000).
[8] D. Aoki, A. Huxley, E. Ressouche, D. Braithwaite, J. Flouquet, J.-P. Brison, E. Lhotel, and C. Paulsen, Nature (London) **413**, 613 (2001).
[9] N. T. Huy, A. Gasparini, D. E. de Nijs, Y. Huang, J. C. P. Klaasse, T. Gortenmulder, A. de Visser, A. Hamann, T. Görlach, and H. v. Löhneysen, Phys. Rev. Lett. **99**, 067006 (2007).
[10] A. Krimmel, P. Fischer, B. Roessli, H. Maletta, C. Geibel, C. Schank, A. Gauel, A. Loidl, and F. Steglich, Z Phys. B Condens. Matter **86**, 161 (1992).
[11] R. Caspary, P. Hellmann, M. Keller, G. Sparn, C. Wassilew, R. Köhler, C. Geibel, C. Schank, F. Steglich, and N. E. Phillips, Phys. Rev. Lett. **71**, 2146 (1993).
[12] M. Jourdan, M. Huth, and H. Adrian, Nature (London) **398**, 47 (1999).
[13] N. Metoki, Y. Haga, Y. Koike, and Y. Onuki, Phys. Rev. Lett. **80**, 5417 (1998).
[14] N. Bernhoeft, N. Sato, B. Roessli, N. Aso, A. Hiess, G. H. Lander, Y. Endoh, and T. Komatsubara, Phys. Rev. Lett. **81**, 4244 (1998).
[15] N. Bernhoeft, Eur. Phys. J. B **13**, 685 (2000).
[16] N. K. Sato, N. Aso, K. Miyake, R. Shiina, P. Thalmeier, G. Varelogiannis, C. Geibel, F. Steglich, P. Fulde, and T. Komatsubara, Nature (London) **410**, 340 (2001).
[17] C. Geibel, A. Böhm, R. Caspary, K. Gloss, A. Grauel, P. Hellmann, R. Modler, C. Schank, G. Weber, and F. Steglich, Physica (Amsterdam) **186–188B**, 188 (1993).
[18] Y. Haga, Y. Inada, K. Sakurai, Y. Tokiwa, E. Yamamoto, T. Honma, and Y. Onuki, J. Phys. Soc. Jpn. **68**, 342 (1999).
[19] Y. Inada, H. Yamagami, Y. Haga, K. Sakurai, Y. Tokiwa, T. Honma, E. Yamamoto, Y. Onuki, and T. Yanagisawa, J. Phys. Soc. Jpn. **68**, 3643 (1999).
[20] L. M. Sandratskii, J. Kübler, P. Zahn, and I. Mertig, Phys. Rev. B **50**, 15834 (1994).
[21] K. Knöpfle, A. Mavromaras, L. M. Sandratskii, and J. Kübler, J. Phys. Condens. Matter **8**, 901 (1996).
[22] G. Zwicknagl, A. Yaresko, and P. Fulde, Phys. Rev. B **68**, 052508 (2003).
[23] M. Kyogaku, Y. Kitaoka, K. Asayama, C. Geibel, C. Schank, and F. Steglich, J. Phys. Soc. Jpn. **62**, 4016 (1993).
[24] H. Tou, Y. Kitaoka, K. Asayama, C. Geibel, C. Schank, and F. Steglich, J. Phys. Soc. Jpn. **64**, 725 (1995).
[25] See for the general implications on possible pairings of this symmetry operation: M. Ozaki and K. Machida, Phys. Rev. B **39**, 4145 (1989).
[26] T. Watanabe, K. Izawa, Y. Kasahara, Y. Haga, Y. Onuki, P. Thalmeier, K. Maki, and Y. Matsuda, Phys. Rev. B **70**, 184502 (2004).
[27] G. E. Volovik, JETP Lett. **58**, 469 (1993).
[28] P. Miranović, N. Nakai, M. Ichioka, and K. Machida, Phys. Rev. B **68**, 052501 (2003).
[29] P. Miranović, M. Ichioka, K. Machida, and N. Nakai, J. Phys. Condens. Matter **17**, 7971 (2005).
[30] I. Vekhter, P. J. Hirschfeld, J. P. Carbotte, and E. J. Nicol, Phys. Rev. B **59**, R9023 (1999).
[31] T. Sakakibara, A. Yamada, J. Custers, K. Yano, T. Tayama, H. Aoki, and K. Machida, J. Phys. Soc. Jpn. **76**, 051004 (2007).
[32] K. An, T. Sakakibara, R. Settai, Y. Onuki, M. Hiragi, M. Ichioka, and K. Machida, Phys. Rev. Lett. **104**, 037002 (2010).
[33] S. Ikeda, H. Shishido, M. Nakashima, R. Settai, D. Aoki, Y. Haga, H. Harima, Y. Aoki, T. Namiki, H. Sato, and Y. Onuki, J. Phys. Soc. Jpn. **70**, 2248 (2001).
[34] $H_{c2}$ has been reported to be slightly anisotropic but almost the same in the hexagonal plane [26,35]: $H_{c2}$ at 0.4 K are 3.12 T and 3.2 T for $H\|[10\bar{1}0]$ and $H\|[11\bar{2}0]$, respectively ($H_{c2}^{[10\bar{1}0]} \lesssim H_{c2}^{[11\bar{2}0]}$). $H_{c2}$ at 0.20 K is expected to be larger than that at 0.40 K, but the temperature dependence of $C(T)/T$ does not show the jump at the SC transition at 4 T for $H\|[11\bar{2}0]$ down to 0.1 K [Fig. 1(a)], indicating that the system is not in the SC state but in the normal (AF) state at 4 T.
[35] Y. Haga, E. Yamamoto, Y. Inada, D. Aoki, K. Tenya, M. Ikeda, T. Sakakibara, and Y. Onuki, J. Phys. Soc. Jpn. **65**, 3646 (1996).
[36] Assuming the effective mass model, the polar-angle dependence of $H_{c2}$ is described as follows: $[H_{c2}(\theta)/H_{c2}(0°)] = (\Gamma/\sqrt{\Gamma^2\cos^2\theta + \sin^2\theta})$, where $\Gamma \equiv [H_{c2}(90°)/H_{c2}(0°)]$. Note that the field variation of the Sommerfeld coefficient of a superconductor can be written as $\gamma(H) \propto [H/H_{c2}]^\beta$, where $\beta = 1$ and $1/2$ for full-gap and line nodal superconductors, respectively. We thus obtain $\gamma(\theta) \propto [H/H_{c2}(\theta)]^\beta = A[\Gamma^2\cos^2\theta + \sin^2\theta]^{\beta/2}$, where $A$ is a constant. Irrespective of the value $\beta$, $\gamma(\theta)$ is a monotonic function of $\theta$, and does not give a local maximum around $\theta = 30$–$60°$.
[37] Y. Nagai, H. Nakamura, and M. Machida, Phys. Rev. B **83**, 104523 (2011).
[38] Y. Tsutsumi, T. Nomoto, H. Ikeda, and K. Machida, arXiv:1604.02806.
[39] M. Sigrist and K. Ueda, Rev. Mod. Phys. **63**, 239 (1991).
[40] The realizability of this two-dimensional representation state is discussed in M. Ozaki and K. Machida, J. Phys. Soc. Jpn. **61**, 2665 (1992); **61**, 4671B (1992).